

# Data Processing in Cellular Microphysiometry

Joachim Wiest\*, *Senior Member, IEEE*, Aldric Namias, Cornelia Pfister, Peter Wolf, Franz Demmel, and Martin Brischwein

**Abstract—Goal:** This contribution points out the need for well-defined and documented data processing protocols in microphysiometry, an evolving field of label-free cell assays. The sensitivity of the obtained cell metabolic rates toward different routines of raw data processing is evaluated. **Methods:** A standard microphysiometric experiment structured in discrete measurement intervals was performed on a platform with a pH- and O<sub>2</sub>-sensor readout. It is evaluated using three different data evaluation protocols, based on A) fast Fourier transformation of such dynamics, B) linear regression (LIN) of pH(t) and O<sub>2</sub>(t) dynamics, and C) numerical simulation (SIM) with a subsequent fitting of dynamics for parameter estimation. **Results:** We propose a sequence of well documented steps for an organized processing of raw sensor data. Figures of merit for the quality of raw data and the performance of data processing are provided. To estimate metabolic rates, a reaction-diffusion modeling approach is recommended if the necessary model input parameters such as the distribution of the active biomass, sensor response time, and material properties are available. **Conclusion:** The information about cellular metabolic activity contained by measured sensor data dynamics is superimposed by manifold sources of error. Careful consideration of data processing is necessary to eliminate these errors as much as possible and to avoid an incorrect interpretation of data.

**Index Terms—**Biomedical transducers, data processing, Fourier transforms, metabolism, microphysiometry, micro-sensors, oxygen, pH, reaction-diffusion modeling.

## I. INTRODUCTION

THE term “microphysiometry” was introduced by McConnel *et al.* to describe measurements of extracellular acidification rates (EAR) with the then newly invented “silicon microphysiometer” [1]. Since then, the measurement of EAR with pH sensors and oxygen uptake rates (OUR) with dissolved oxygen sensors has become a well-accepted research tool for cell biology, using both electrochemical (see, e.g., [2]–[5]) and optochemical [see, e.g., [6], [7]) sensor technology. In addition to pH and dissolved O<sub>2</sub>, the monitoring of metabolites with sensors for glucose and lactate comes into focus [4], [8], [9]. The capability to study the metabolic dynamics of unlabeled cellular specimens in real time and continuously for hours or days, accounts for the value of this approach. Thanks to the generality of the measured parameters, a wide spectrum of cellular objects spanning from bacteria, unicellular algae [10], cell lines, stem cells [11], and interacting microphysiological systems [12] can be analyzed without any prior knowledge of pathways that

might be involved in the response to an experimental treatment. There are now efforts to apply microphysiometry to organotypic tissue models of solid human cancers as a building block of personalized tumor medicine [13], [14]. At the latest it will be this point, where validated methods of data processing and signal analysis will be asked for—with good reason, since therapeutic decisions might rely on the test results.

Until now, EAR and OUR data are derived from pH(t) and O<sub>2</sub>(t) plots measured by an interval sampling consisting of a rapid medium exchange event followed by a rest time interval. The decline rate dpH/dt and dO<sub>2</sub>/dt of the parameters in the rest time interval, due to metabolic acidification and oxygen consumption and determined by plain linear regression (“LIN”), is taken as an approximate measure of EAR and OUR.

However, this approximation may become risky if the numerous sources of error are not adequately considered [9]. For example, if the environmental conditions are changing during the rest time interval (e.g., by user interaction), the actual EAR and OUR may vary in response to the disturbance. Second, the linear approximation of dpH/dt and dO<sub>2</sub>/dt disregards any curvature that is due to variable cell activities, reaction and diffusion processes with inhomogeneous distributions of the active biomass, and slow sensor responses. These factors, next to effects of noninert materials confining the measurement setup and buffering of pH can be considered in a model-based approach providing a rational basis for the estimation of absolute values of EAR and OUR [15], [16].

This model- and simulation-based approach (“SIM”) is one of the three data processing options presented here. As long as absolute rate values are not the prime interest and the recording of relative changes in the course of an experiment is sufficient (implying some kind of normalization of rate values at an arbitrary reference point of time), the LIN method may be applicable. As an advancement, we present a data processing protocol that includes a filtering of the pH(t) and O<sub>2</sub>(t) plots in the frequency domain in order to eliminate sensor drift and noise and to enhance the extraction of metabolic rate values from raw data plots (named “FFT,” since a fast Fourier transformation is involved).

To evaluate these different methods of data processing, an experimental protocol on a microphysiometric platform involving the treatment of cell cultures with an agent of well-defined effect has been chosen. This experiment was run three times to include an assessment of (intralab) reproducibility. The criterion chosen to rate the data processing methods is essentially based on the separation of the metabolic rates obtained from “treated” cultures compared to untreated control cultures.

The central question to be addressed in this study is: How can the requested cell metabolic rates—or at least the relative changes of such rates during the course of an experiment—be derived in a transparent, unambiguous, and rational way from

Manuscript received November 9, 2015; accepted February 18, 2016. Date of publication February 23, 2016; date of current version October 18, 2016. Asterisk indicates corresponding author.

\*J. Wiest is with the cellasys GmbH-R&D, Munich 80802, Germany (e-mail: wiest@cellasys.com).

A. Namias and Martin Brischwein are with the Technische Universität München, Heinz Nixdorf - Lehrstuhl für Medizinische Elektronik.

C. Pfister, P. Wolf, and F. Demmel are with the HP Medizintechnik GmbH. Digital Object Identifier 10.1109/TBME.2016.2533868

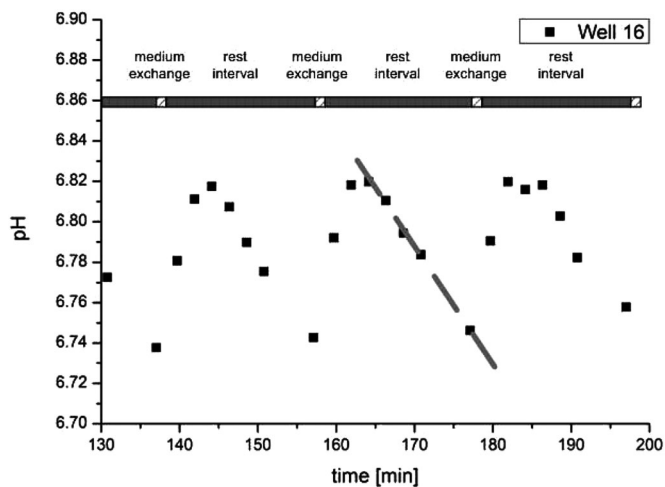


Fig. 1. Raw data dynamics (rectangles) of a pH microsensors in a microscaled cell culture chamber, reflecting the regular fluid cycles: Fresh cell culture medium is transported into the chamber during the exchange intervals causing an increase of pH. In the following rest interval, cellular acid extrusion leads to a decline of pH. The dashed grey line is a linear regression fitted to the sensor data in one of the rest intervals to calculate a rate value  $\text{dpH}/\text{dt}$ .

the measured raw sensor data dynamics? So far, this aspect has only received incidental treatment in the literature. This work should help to establish standard operation procedures and figures of merit for the layout and data evaluation of microphysiometric experiments.

## II. MATERIALS AND METHODS

### A. General Microphysiometric Setup

From the very beginnings of microphysiometric cell assays, an exchange and rest interval of the involved fluidic system with regular timestamps has become widely accepted. This system transports cell culture media in an alternating exchange—and rest interval through “micro reaction volumes” (MRVs) where the specimens are trapped and cultured. Such microscaled volumes are clearly preferred in order to achieve a sufficient sensitivity and speed of the monitoring process, to limit the consumption of valuable chemical compounds in the media and to reduce the required cell number or tissue biomass (which may also be limited).

Changes of the extracellular environment due to the activity of cellular core metabolism—i.e., decreasing pH values and dissolved oxygen concentrations—will occur during the rest intervals while the exchange intervals are necessary to re-establish the known conditions of the fresh medium (see Fig. 1) [14]. The duration of the rest intervals should be adjusted to avoid large deviations of pH and  $\text{O}_2$  beyond preset limits of tolerance. Such segmentation into distinct measurement intervals allows a frequent sampling of “metabolic rates” without a long-term deterioration of the culture media and a control of sensor drift since the known conditions of fresh culture medium are adjusted after every flow interval. The result is a line chart of EAR and OUR for each sensor in each of the cell cultures.

### B. Experimental Protocols

To test the analysis of microphysiometric data in practice, a recently developed label free cell assay platform [17] was used. The core of that platform is a test plate with 24 independent MRVs, each with an optochemical sensor spot for pH and dissolved oxygen (PreSens GmbH, Regensburg, Germany) placed on a transparent polymer bottom sheet. Each MRV is connected with two adjacent containments providing access to the fluidic system.

The L929 mouse fibroblast cell line was cultured in Dulbecco’s modified eagle medium (DMEM) containing 5% heat inactivated fetal calf serum, 4.5 g/L glucose, 4 mM L-glutamine and 3.7 g/L sodium bicarbonate (culture medium) in a standard cell incubator (95% humidity, 37 °C, 10%  $\text{CO}_2$ ). Cells were seeded into the wells of the test plate (75.000/well) and incubated 6 h under standard conditions for cellular attachment. After this incubation, the medium was replaced by an unbuffered running medium (DMEM, 5% heat inactivated fetal calf serum, 4.5 g/L glucose, 4 mM L-glutamine) to enable the detection of extracellular acidification.

The plate was closed with its cover lid confining the 24 MRVs, plugged into the instrumental platform and the experimental protocol was started. Every 20 min the pipetting robot exchanges the medium in the MRVs to apply fresh media and/or drugs. The 48 optochemical sensors are read out sequentially every 120 s (sampling rate  $8 \cdot 10^{-3}$  Hz) with an inverse process microscope mounted on a x-/y-stage beneath the test plate.

After 12 h under standard conditions (running medium without additional agents), the test compound sodium lauryl sulfate (SLS) was added for another 12 h to the treated groups. SLS is an anionic surfactant (detergent) which is widely used as a positive control or standard compound in cytotoxic tests [18]. Two different concentrations were applied to achieve an instantaneous cytotoxic effect (778  $\mu\text{g}/\text{ml}$ ) and a moderately cytotoxic effect (77.8  $\mu\text{g}/\text{ml}$ ). Finally, all cultures (including the previously untreated negative control) were lysed with 0.2% Triton X-100 in running medium (positive control).

Three experiments were performed according to the same protocol, denoted with numbers “{1},” “{2},” and “{3}.” The protocol includes differently treated groups of cell cultures along with an untreated (control) group, the number  $n$  of cell cultures in each group is  $n = 6$ . In the following, only pH and EAR data are shown since the treatment of  $\text{O}_2$  – (OUR) data is analogous [16].

### C. Description of Data Analysis

A sequence of three main steps is identified to process the raw data derived from a microphysiometer. As outlined earlier, three different options to evaluate the raw data derived from a microphysiometer are considered and compared (see Fig. 2): A) Filtering in the frequency domain and amplitude determination (FFT), B) linear regression (LIN) and C) parameter estimation supported by simulated sensor dynamics (SIM).

The data processing is organized into four consecutive steps. Starting point is a panel of raw data dynamics corresponding to the experimental layout with differently treated groups of cell

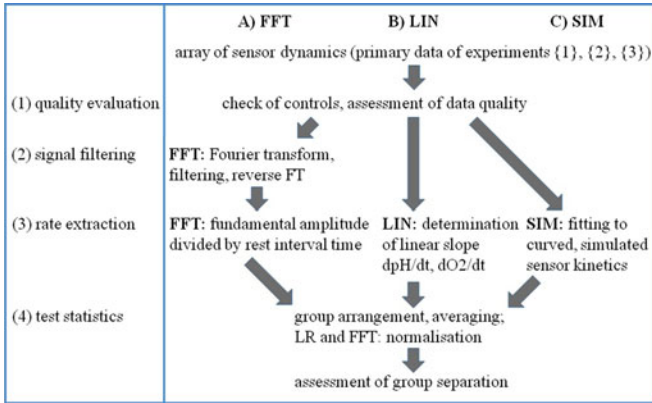


Fig. 2. Workflow of data treatment steps. Starting point is a panel of sensor dynamics resulting, e.g., from the experimental layout of a test plate. Quality evaluation and test statistics are procedures common to all data evaluation routines. The way of signal filtering and rate extraction is characteristic for each of the methods described here.

cultures. Each of these dynamics are segmented into intervals as described above for the general microphysiometric setup.

*Step 1: Quality valuation:* A first quality check of an experiment will consider the positive and negative controls. As a positive control, an agent is applied to the cell cultures that will safely and quickly destroy any viability. Only those experiments pass this checkpoint, where the activity of untreated cultures (= negative controls) falls below a predefined threshold after addition of this agent.

Prior to downstream data treatment, a correction of outliers may be appropriate, e.g., according to Dixon [19]. However, this correction is controversially discussed since it depends on an arbitrary setting of thresholds.

The quality of the data refers to the variability or superimposed “noise” in the rate line charts. It is anticipated, that cell metabolic rates of untreated cultures in equilibrium conditions are constant within the time scale of some hours. The leading cause of rate noise is a noisy sensor in combination with a low sensor readout frequency or data sampling rate. Other sources of noise such as air bubbles in the fluidic system may also lower the reliability of the data.

A criterion to verify data quality can be derived similar to a signal to noise ratio. The noise can be estimated by comparison of the slopes in the  $pH(t)$  and  $O_2(t)$  plots in different measurement intervals. Formula 1 describes the procedure. A time point of the previous measurement interval  $D_{i-1}$  is subtracted from the same time point in the actual measurement interval  $D_i$ . The sum  $Q$  is the division of the signal and the calculated differences. It provides a factor related to the quality (i.e., stability) of the measurement values,

$$Q = \sum \frac{D_i^2}{(D_i - D_{i-1})^2}. \quad (1)$$

One of the available options to take into account different data qualities is the introduction of such parameters as a weight factor assigned to different cell culture wells for the downstream statistical data evaluation. Here, however  $Q$  is

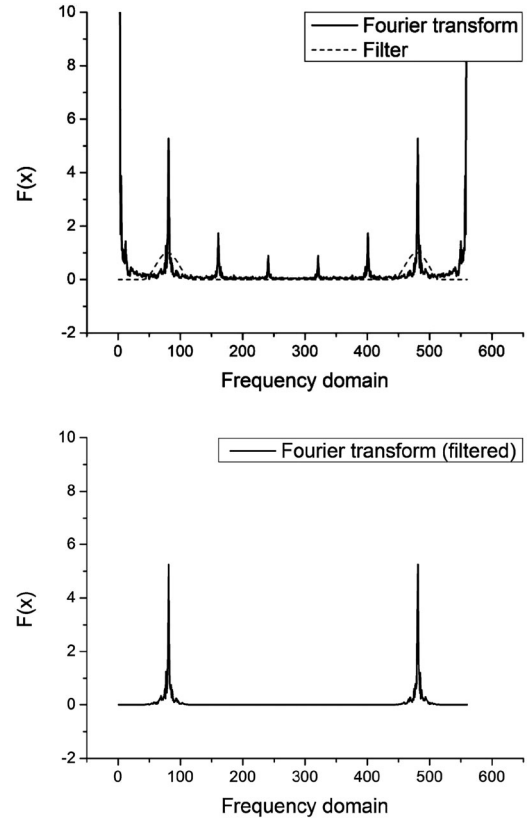


Fig. 3. Top: Frequency domain of well 16 (straight) and filter (grey, dashed). Bottom: Frequency domain after convolution with filter. The corresponding time domain is plotted in Fig. 5.

used as a threshold value to exclude sub-threshold culture wells from further evaluation.

*Step 2: Signal filtering:* The basic mathematical procedure is a filtering of dynamic sensor plots in the frequency domain by FFT to separate the relevant data concentrated in a narrow frequency domain from irrelevant or erroneous data in the low- and high-frequency part of the spectrum. With respect to the low-frequency part, sensor drift may compromise the measurement. With respect to the high-frequency part, white noise adds to the raw signal.

The exact relevant frequency domain is still unknown, but it can be approximated by using the shape of the fluid cycles translated into the frequency domain. The obtained spectrum is multiplied by a predefined filter. The inverse FFT brings the filtered data back to the time domain.

The idea behind the FFT method is that all relevant microphysiometric information must be in the frequency domain of the medium exchange/rest interval periodicity. The data in the frequency domain presents peaks at the fluid cycle frequency and at its harmonics. To eliminate noise from other frequency domains, the chosen pass band is the proximity of the highest peak, with cosines attenuation (see Fig. 3 top). The width of the pass band is the distance between peaks. Only the fluid cycle frequency but not its harmonics is allowed by the filter.

*Step 3: Rate extraction:* The (optional) signal filtering in the frequency domain is followed by a data reduction step since now each measurement interval will be assigned a single rate value in units of  $\Delta\text{pH}/\text{s}$  and  $\Delta\text{O}_2/\text{s}$ . Notably, this single rate value may be a simplification in case of rate variations *within* a rest interval. Three different options for this step are identified:

- 1) Assessment of the amplitude  $\Delta\text{pH}$  and  $\Delta\text{O}_2$  (or the fundamental amplitude in case of a prior frequency filtering) divided by the length  $\Delta t$  of the measurement interval. This is applied in the FFT approach.
- 2) Assessment of the slope  $\text{dpH}/\text{dt}$  and  $\text{dO}_2/\text{dt}$  in each rest interval calculated by linear regression (see dashed line in Fig. 1), as realized in the LIN approach (here without prior signal filtering); LIN can be constrained to an initial part of the rest interval.
- 3) Fitting to sensor dynamics calculated by numerical modeling (SIM approach).

Briefly, in the SIM method, a finite element model (FEM) was set up describing the metabolic activity within an MRV, including all relevant transport processes like diffusion and buffer effects, and sensor response characteristics [13]. The aim is to yield a set of synthetic sensor dynamics. Fitting these synthetic dynamics to experimental dynamics provides an estimation of the required EAR. There is no filtering or smoothing of experimental sensor dynamics prior to the fitting of measured sensor dynamics to the simulated dynamics since this would be in conflict with the correct physical model underlying the simulation.

The reaction-diffusion model was set up in COMSOL Multiphysics 4.3b (COMSOL Multiphysics GmbH, Goettingen, Germany) and MATLAB Simulink (The MathWorks Inc., Natick, MA, USA). The FEM was set up with a range of discrete values for EAR stored in a database. For simplifying the process, the EAR is assumed as constant within individual measurement intervals. The measured sensor dynamics for each cell culture and measurement interval were fitted by a least square fit to the synthetic sensor dynamics and the dynamics with the best fit to the measured data was chosen to estimate the EAR. Notably, this method yields EAR values in units of molar flux (moles  $\text{H}^+/\text{m}^2\cdot\text{s}$  secreted) instead of  $\text{pH}/\text{s}$  since the buffer capacity  $\beta(\text{pH}) = -\text{dc}(\text{H}^+)/\text{dpH}$  is taken into account. In this model, a constant value of  $\beta$  is assumed for the complete range of  $\text{pH}$  to facilitate the calculations. In general, however, we strongly recommend to quantify the function  $\beta(\text{pH})$  by own measurements. In case the occurring  $\text{pH}$  values exceed the range where the assumption of  $\beta$  as a constant is considered to be valid, the measured function  $\beta(\text{pH})$  should be included into the model. A suitable way to do this is to implement a lookup table where the simulation accesses the appropriate values of  $\beta$  at each iteration step. Owicki and Parce further expound on the physical chemistry and cell biology of extracellular acidification [20].

*Step 4: Test statistics:* Cellular activity measured from the culture wells of each differentially treated group is averaged and standard deviations are calculated. To account for the variability of activity values among the culture wells, these averaged rates and related standard deviations may be normalized. They are set to unity (e.g., 100%) at a selected reference time point, reasonably at the time of drug addition. To reduce the impact of potential outliers in the averaged group, the mean of activity values 1 h before the reference time point is considered for normalization.

A statistical treatment requires an experimental layout providing treated and untreated groups of culture wells. To derive a quantitative measure of probability of a treatment-related effect, a statistical test must be applied. Assuming a normal distribution with equal sizes of samples in the groups, a Student's t-test (two-tailed and unpaired t-test of treated against untreated) can be applied for every measurement interval. However, since a test of normal distribution is questionable with an  $n = 6$ , a different measure was chosen.

Since the outcome of the experiment is known, a (normalized) rate value of 1 is expected for the control group during the time of treatment ( $t = 12\text{--}24$  h) while the expected rate value for the group treated with  $778 \mu\text{g}/\text{ml}$  SDS is 0 in that period. To assess the performance of the different routes of data processing, a mean square error (MSE) was calculated (2) with a distinct rate value at time  $t(M_t)$ , the expected value at time  $t(M_{E,t})$ , and standard deviation at time  $t(\sigma_t)$ . In order to increase the data basis of that figure of merit, the mean of a time period containing  $n$  measurement intervals between the start ( $t_S = 18$  h) and the end ( $t_E = 22$  h) of the calculation is selected to obtain the MSE. The higher the real outcome deviates from the expected result of the experiment, the higher the MSE value gets. The parameter is used to compare the performance of the different methods

$$\text{MSE}_t = \frac{1}{n} \sum_{t_S}^{t_E} \left[ (M_t - M_{E,t})^2 \sigma_t \right]. \quad (2)$$

### III. RESULTS

#### A. Application of Data Analysis Protocols to a Given Set of Micophysiometric Data

This section shows the execution of the data treatment methods described earlier toward a concrete set of micophysiological experiments that have been performed with the assay platform as described in Section II-A. All data shown result from  $\text{pH}$  sensor measurements yielding EAR values.

*Step 1: Quality valuation:* The validity analysis of the  $\text{pH}$ -sensor's raw data dynamics yields widely differing  $Q$  values (see Fig. 4). When a threshold of  $Q = 10^5$  is set, in  $\{2\}$ , no invalid wells were identified. Thus, subsequent data processing steps are performed on data from  $\{2\}$ . The invalidation of wells below the threshold of  $\{1\}$  (well 3, 5, and 11) and  $\{3\}$  (well 6) corresponded to notes by the operator (e.g., insufficient cell density). The threshold has to be set empirically, yet the exclusion or inclusion of culture wells is determined on a rational basis.

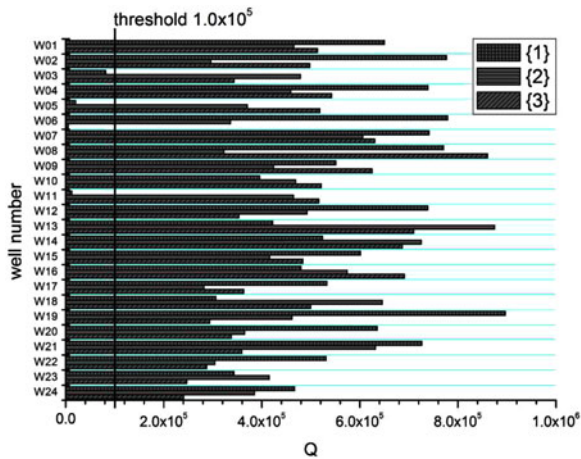


Fig. 4. Quality weighting of the three experiments (top: {1}, middle: {2}, bottom: {3}). Wells with  $Q$  values below the threshold of  $10^5$  are excluded from further processing.

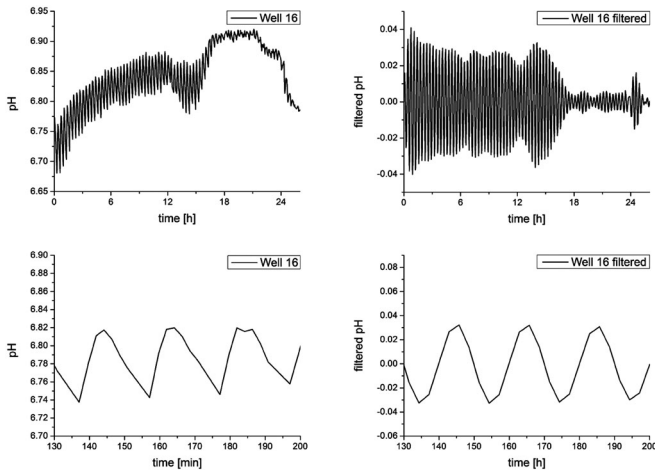


Fig. 5. Effect of signal filtering with a frequency band centered at the frequency of medium-exchange ({2}, well 16). Left: unfiltered, right: filtered. Below: details as in Fig. 1. Please note that the indicated acidity of the medium ( $\text{pH} \approx 6, 7$ ) results from the inaccuracy of sensor calibration: The  $\text{pH}$  of the culture medium was adjusted to  $\text{pH} = 7, 4 (+/- 0, 1)$ .

**Step 2: Signal filtering:** The effect of filtering essentially is the elimination of both noise and drift. In Fig. 5, an example from {2}, well #16,  $\text{pH}$ -sensor, is shown. Here, e.g., the sensor drift (top, left) is removed by filtering.

**Step 3: Rate extraction:** When forward and inverse FFT are applied, the fundamental amplitude  $\text{pH}_{\text{max}} - \text{pH}_{\text{min}}$  (divided by  $\Delta t$ ) yields a measure of EAR (FFT method). Alternatively, the unfiltered raw sensor data in the rest intervals are analyzed by linear regression to obtain a slope  $\text{dpH}/\text{dt}$  as a measure of EAR (LIN method).

With the SIM method, the EAR yielding the best fit to the measured sensor dynamics are selected from the base data containing values of EAR ranging from 0 to  $0.4 \mu\text{mol H}^+ / (\text{m}^2\text{s})$  per well. Fig. 6 shows an example of experimental and fitted  $\text{pH}$  sensor dynamics.

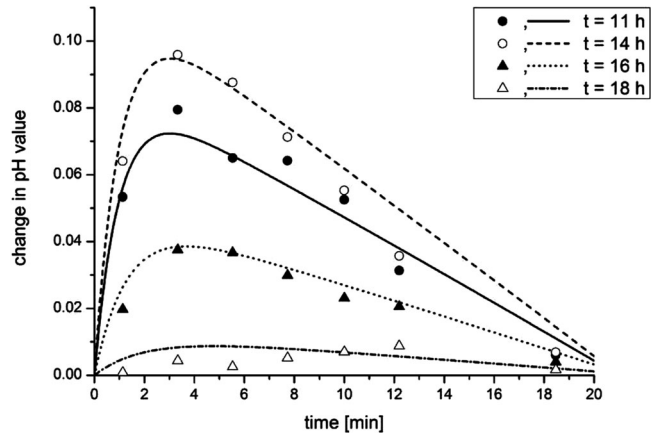


Fig. 6. Comparison between the measured (single points) and the simulated (lines)  $\text{pH}$  values for four 20-min measurement intervals at four different times. The  $\text{pH}$  values were normalized by a baseline cutoff to the endpoint of the intervals. Thus, only changes in the  $\text{pH}$  values are plotted. The exchange of the medium in the MRV at the beginning of an interval goes along with an increase of  $\text{pH}$ , the following decrease is caused by the EAR of the cells. The calculated graphs of the analyzed rest intervals are in good agreement with the measured data.

**Step 4: Test statistics:** Equally treated culture wells of an experiment are arranged into groups and averages of EARs are calculated for all three methods of data processing. As described earlier, the means over a time span of 1 h prior to of drug addition was considered for normalization. Fig. 7 shows the EAR plots of experiment {2} that result from methods FFT, LIN, and SIM.

Table I provides the MSEs calculated for the three different data processing routines at time 18–22 h of the assay. The treated group was the one receiving  $778 \mu\text{g}/\text{ml}$  SDS. A lower MSE value means a better compliance of the predicted and the measured values, indicating a higher performance of data evaluation.

#### IV. DISCUSSION

In the ideal case, the dynamic sensor measurements of  $\text{pH}$  and  $\text{O}_2$  are equivalent to the real dynamics  $\text{pH}(t)$  and  $\text{O}_2(t)$ .

However, the measured sensor data are typically compromised by noise, low sampling frequency, slow sensor response time, and signal drift. This requires a methodological reflection about 1) how to reconstruct absolute cell metabolic rates from such superimposed sensor data and 2) how the relative changes of these rates can be mapped correctly.

Despite the numerous sources of error in the simulation (e.g., uncertainty about the correct diffusion constants and response time of sensors) requiring a multivariate fitting to the—likewise impaired—experimental data: a theory-based validated model appears to be the best choice for estimating absolute metabolic rates from the data. If the local distribution of active biomass within an MRV is assessable, an additional yield of such a model is the information about the spatiotemporal evolution of  $\text{pH}$  and  $\text{O}_2$  values which may be particularly important for the maintenance of tissue slices [16].

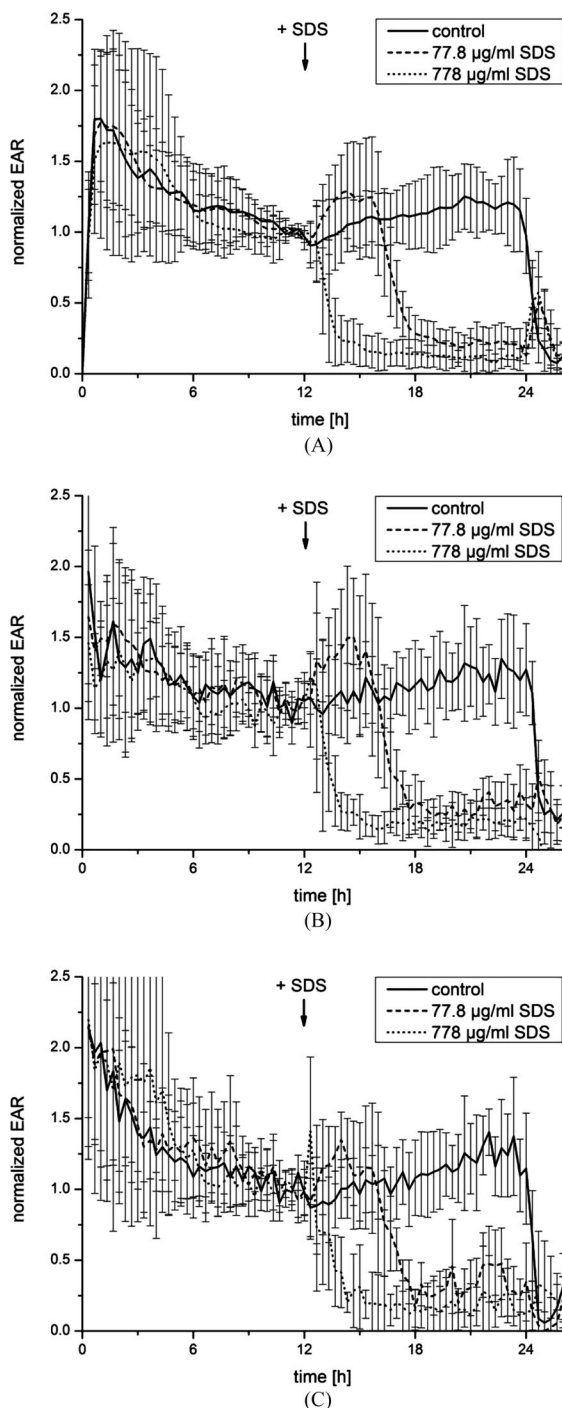


Fig. 7. Plots of EAR estimates according to methods FFT, LIN, SIM (see Fig. 2) of experiment {2} after arrangement in groups, averaging, and normalization (straight: negative control, dashed: 77.8  $\mu\text{g/ml}$  SLS, dotted: 778  $\mu\text{g/ml}$  SLS). (A) FFT. (B) LIN. (C) SIM.

A determination of metabolic rates by FFT and LIN were feasible only if the sensor response is fast compared to the rest interval time and if the metabolic activity is nearly constant within the rest intervals. Provided that the absolute rates can be determined from the raw data, a correct plot of *relative* changes in the course of an experiment—which are central to many

TABLE I  
CALCULATED MSE OF FFT, LIN, AND SIM

	A) FFT	B) LIN	C) SIM
Control	8.22E-3	14.72E-3	10.02E-3
778 $\mu\text{g/ml}$ SDS	1.40E-3	3.75E-3	7.08E-3

pharmaceutical or toxicological assays—would result automatically. Because of its complexity the model-based approach is hardly pursued, and alternative data processing solutions are required to map these relative changes. It turns out that different *a priori* and equally plausible data processing routines yield similar yet not identical results and the question arises, how to assess the value and performance of these routines.

LIN of  $\text{pH}(t)$  or  $\text{O}_2(t)$  plots is the traditional approach employed by most of the users of microphysiometric devices. The noise reduction of the FFT method toward microphysiometric data is, to our knowledge, described for the first time. From a signal processing point of view, SIM has been developed to estimate spatio-temporal profiles of  $\text{pH}$  and  $\text{O}_2$  in MRVs. Using the MSE criterion defined above, FFT shows an improvement of LIN for the presented dataset.

However, we advise against a generalization of this finding since the outcome of a comparison will depend on the fine adjustments of the protocols. Filtering, e.g., by smoothing or nonlinear regression was not applied at all in the LIN routine and the selected filter parameters in the FFT protocol have not been optimized systematically. In addition, the determination of cycle amplitudes by FFT will underestimate the metabolic rates as soon as the duration of the rest intervals increases and the curvature of  $\text{pH}(t)$  and  $\text{O}_2(t)$  plots becomes prominent.

As outlined earlier, there are problems where the knowledge of absolute metabolic rates, e.g., in terms of moles  $\text{O}_2/\text{s}$  consumed or moles  $\text{H}^+/\text{s}$  excreted per cell culture well is important (see, e.g., [21], [22]). Here, a careful elimination of sensor response characteristics, ( $\text{pH}$ -) buffering and material effects is indispensable and argues for the use of a numerical (reaction-diffusion) model to simulate the sensor dynamics. With respect to the elimination of (oxygen) gas binding effects to materials surrounding the MRVs (becoming particularly important at high surface to volume ratios), an alternative compartment model-based correction algorithm has been described [23]. The simulation based on our reaction-diffusion model is followed by parameter estimation, i.e., fitting of the simulated sensor dynamics to the experimental ones. Unfortunately, the precision of the metabolic rates obtained is limited by the accuracy of a number of input variables. These variables include the diffusion constants, sensor response times, and the knowledge about the spatial and temporal distribution of cell activity within the MRV. Thus, the accuracy of the fitting procedure is impaired by a multitude of degrees of freedom.

The exchange and rest intervals of the fluidic system requires a careful tradeoff between the precision of rate determination, which is promoted by large drops of  $\text{pH}$  and  $\text{O}_2$  within the measurement intervals, and the homeostasis of the cellular

microenvironment. As can be shown with reaction-diffusion models, steep gradients of pH and  $O_2$  can arise during the stop intervals in cultures of tissue slices or organoids, where convective transport in the exchange intervals is restricted to the exterior of the tissue culture [16]. Apart from these considerations, the length of the measurement intervals also sets the limit of time resolution of detecting fast changes in cellular activity. Thus, a requirement for the measurement platform and data evaluation protocol is its ability to cope with small amplitudes of  $\Delta pH$  and  $\Delta O_2$ . This in turn asks for short rest intervals and a frequent sampling of raw sensor data. As the Nyquist–Shannon theorem tells us, a signal has to be sampled with a frequency of  $2 \cdot f_{max}$ , (where  $f_{max}$  is the highest wavelet frequency of the original signal) in order to be reconstructed from a discrete sequence of measurements. Since a previous frequency analysis of the pH(t) and  $O_2$ (t) plots (derived from the platform used for this study) yielded maximum frequencies at 10 Hz, the current measurement protocol with a sampling frequency of  $8 \cdot 10^{-3}$  Hz implies a severe undersampling that further limits the precision of signal reconstruction and parameter estimation.

After successful data extraction as described in this study, further data processing such as calculation of metabolic rate decrement by 50% (MRD50) values [18], analysis in Karnaugh maps [24], or division by vehicle control [25] are useful tools to further extract information from microphysiometric systems.

## V. CONCLUSION

The intention of this study is not to propose a distinct method of data processing but to point out the need for a rational and accurately defined and documented data interpretation procedure. A recommendable approach is the selection of one or two different methods (depending on the intention of data evaluation) followed by a learning phase using a range of (e.g., filter) parameter settings, with a cluster of drug compounds and cell targets with known outcome of the assay.

## ACKNOWLEDGMENT

The authors would like to thank Dr. S. Haug (TUMStat) for discussion of statistical aspects of the presented work, Dr. F. A. Alexander (cellasys) for proofreading and Prof. Dr. B. Wolf and his team at the *Heinz Nixdorf-Lehrstuhl für Medizinische Elektronik (Technische Universität München)* for sustainable support and fruitful discussion. J. Wiest and A. Namias contributed equally to the article.

## REFERENCES

- [1] H. M. McConnel *et al.*, “The cytosensor microphysiometer: Biological applications of silicon technology,” *Science*, vol. 257, pp. 1906–1912, 1992.
- [2] E. Thedinga *et al.*, “Online monitoring of cell metabolism for studying pharmacodynamic effects,” *Toxicol Appl. Pharmacol.*, vol. 220, no. 1, pp. 33–44, 2007.
- [3] J. Wiest *et al.*, “Cellular assays with multiparametric bioelectronic sensor chips,” *Chimia*, vol. 59, pp. 243–246, 2005.
- [4] A. Weltin *et al.*, “Cell culture monitoring for drug screening and cancer research: a transparent, microfluidic, multi-sensor system,” *Lab Chip*, vol. 14, pp. 138–146, 2014.

- [5] S. E. Eklund *et al.*, “Modification of the Cytosensor microphysiometer to simultaneously measure extracellular acidification and oxygen consumption rates,” *Anal. Chim. Acta*, vol. 496, pp. 93–101, 2003.
- [6] S. Beckers *et al.*, “High-throughput, non-invasive and dynamic toxicity screening on adherent cells using respiratory measurements,” *Toxicol In Vitro*, vol. 24, pp. 686–694, 2010.
- [7] M. Wu *et al.*, “Multiparameter metabolic analysis reveals a close link between attenuated mitochondrial bioenergetic function and enhanced glycolysis dependency in human tumor cells,” *Amer. J. Physiol. Cell Physiol.*, vol. 292, pp. C125–C136, 2007.
- [8] R. M. Pemberton *et al.*, “Fabrication and evaluation of a micro(bio)sensor array chip for multiple parallel measurements of important cell biomarkers,” *Sensors*, vol. 14, pp. 20519–20532, 2014.
- [9] S. E. Eklund *et al.*, “A Microphysiometer for simultaneous measurement of changes in extracellular glucose, lactate, oxygen, and acidification rate,” *Anal. Chem.*, vol. 76, pp. 519–527, 2004.
- [10] J. Wiest *et al.*, “Intelligent mobile lab for metabolics in environmental monitoring,” *Anal. Lett.*, vol. 39, no. 8, pp. 1759–1771, 2006.
- [11] P. Ertl *et al.*, “Lab-on-a-chip technologies for stem cell analysis,” *Trends Biotechnol.*, vol. 32, pp. 245–253, 2014.
- [12] J. P. Wikswo, “The relevance and potential roles of microphysiological systems in biology and medicine,” *Exp. Biol. Med.*, vol. 239, pp. 1061–1072, 2014.
- [13] D. Wlodkovic and J. M. Cooper, “Tumors on chips: Oncology meets microfluidics,” *Curr. Opin. Chem. Biol.*, vol. 14, pp. 556–567, 2010.
- [14] R. Kleinhans *et al.*, “Sensor-based cell and tissue screening for personalized cancer chemotherapy,” *Med. Biol. Eng. Comput.*, vol. 50, pp. 117–126, 2012.
- [15] D. Grundl *et al.*, “Reaction-diffusion modelling for microphysiometry on cellular specimens,” *Med. Biol. Eng. Comput.*, vol. 51, no. 4, pp. 387–395, 2013.
- [16] C. Pfister *et al.*, “Estimation of dynamic metabolic activity in micro-tissue cultures from sensor records with an FEM model,” *Med. Biol. Eng. Comput.*, 2015, <http://dx.doi.org/10.1007/s11517-015-1367-7>
- [17] P. Wolf *et al.*, “Automated platform for sensor-based monitoring and controlled assays of living cells and tissues,” *Biosensors Bioelectron.*, vol. 50, pp. 111–117, 2013.
- [18] The Cytosensor Microphysiometer (CM) Toxicity Test, INVITTOX n° 130, [Online]. Available: <http://ecvam-dbalml.jrc.ec.europa.eu>
- [19] W. J. Dixon, “Analysis of extreme values,” *Ann. Math. Stat.*, vol. 21, pp. 488–506, 1950.
- [20] J. C. Owicki and J. W. Parce, “Biosensors based on the energy metabolism of living cells: The physical chemistry and cell biology of extracellular acidification,” *Biosensors Bioelectron.*, vol. 7, pp. 255–272, 1992.
- [21] A. Kuhnke *et al.*, “Bioenergetics of immune cells to assess rheumatic disease activity and efficacy of glucocorticoid treatment,” *Ann. Rheum. Dis.*, vol. 52, pp. 132–139, 2003.
- [22] B. A. Wagner *et al.*, “The rate of oxygen utilization by cells,” *Free Radical Bio. Med.*, vol. 51, pp. 700–712, 2011.
- [23] A. A. Gerencser *et al.*, “Quantitative microplate-based respirometry with correction for oxygen diffusion,” *Anal. Chem.*, vol. 81, pp. 6868–6878, 2009.
- [24] S. E. Eklund *et al.*, “Multianalyte microphysiometry as a tool in metabolomics and systems biology,” *J. Electroanal. Chem.*, vol. 587, pp. 333–339, 2006.
- [25] L. Kamalian *et al.*, “The utility of HepG2 cells to identify direct mitochondrial dysfunction in the absence of cell death,” *Toxicol In Vitro*, vol. 29, pp. 732–740, 2015.



**Joachim Wiest** (M'05–SM'13) received Dipl.-Ing. and Dr.-Ing. degrees in electronic engineering from Technische Universität München, Munich, Germany.

In 2007, he co-founded cellasys GmbH which offers system solutions for analysis of living cells and is currently its CEO. He is an I.A. Member of EMBS in IEEE, EUSAAT, VDE, DECHEMA, VBIO, Bund der Freunde der Technischen Universität München, NEMEON, and EIKON.



**Aldric Namias** was born in Paris, France. He received the Diplôme d'Ingénieur degree from Télécom Bretagne, Brest, France and the M.Sc. degree in electrical engineering and information technology from the Technische Universität München, Munich, Germany.

During his Master's thesis, he studied methods to score information from cell cultures data. He has already worked in many various domains such as information systems for banks, submarine communications, database and internet services, and LTE

communications.



**Cornelia Pfister** studied mechanical engineering with the Technische Universität München, Munich, Germany.

She is currently with the *Heinz Nixdorf—Lehrstuhl für Medizinische Elektronik (Technische Universität München, Munich, Germany)* and the HP Medizintechnik GmbH, Oberschleißheim, Germany.



**Peter Wolf** received the Diploma degrees in biology from the Technische Universität Darmstadt, Darmstadt, Germany, in 2003, and the Ph.D. degree in “Microelectrode array-based impedance spectroscopy for non-invasive detection of drug effects on MCF-7 breast cancer cells” at the Centre for Biotechnology and Biomedicine, BBZ, University of Leipzig, in 2008.

He was founded as Junior Research Fellow by the German Research Council (DFG, *Deutsche Forschungsgemeinschaft*). Since 2009, he has been with the HP Medizintechnik GmbH, Oberschleißheim, Germany, in a project developing and evaluating an automated platform for real-time monitoring of cell-based assays.



**Franz Demmel** studied electrical and computer engineering with the Technische Universität München, Munich, Germany.

As a Research Associate at the Heinz Nixdorf Chair for Medical Electronics, he deals with the conceptual design and the technical realization of a novel high-content screening system with a focus on optochemical sensor technology and microscopy.



**Martin Brischwein** received the Diploma and Ph.D. degrees in biology from Albert-Ludwigs-Universität, Freiburg, Germany.

From 1999 to 2001, he was at the Institute of Biophysics, University of Rostock, Germany. Since then, he has been an Assistant Professor at the Department for Medical Electronics, Technische Universität München. His primary area of research and development is microphysiometry on cells and tissues with electrochemical and optochemical sensors.